

Fig. 7-1. Time-zero measurement taken before the acetophenone experiment. The (a) ellipticity and (b) vertical profile of the electron beam are measured while stepping the delay of the laser excitation with respect to the electron pulses. The point at which electron beam distortion is observed defines time-zero. The measurement, taken on the left (1350 ps) and right (1370 ps) sides of the detector determine the time-zero at the center (1360 ps).

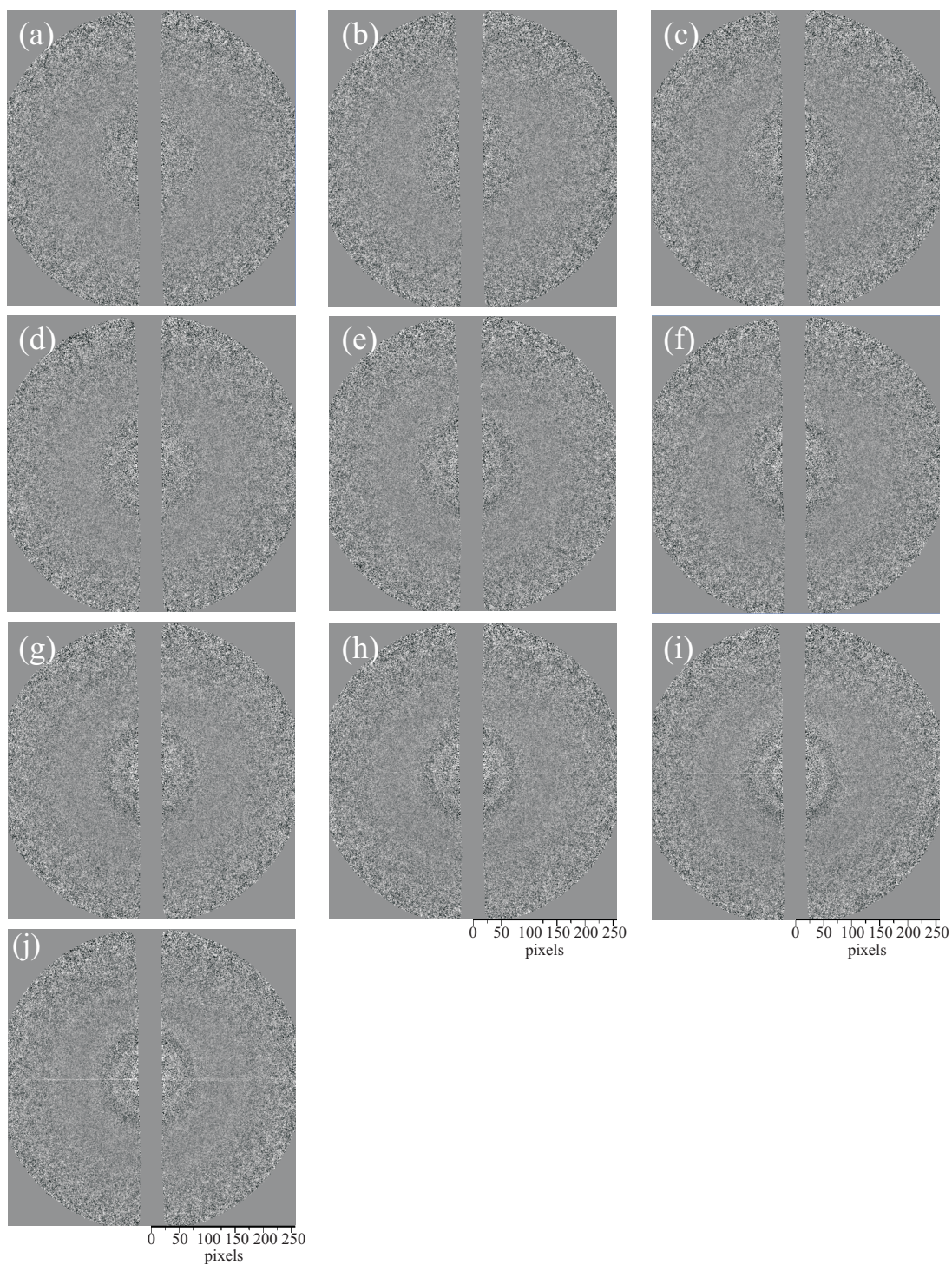


Fig. 7-2. The frame-referenced difference patterns ($t_{\text{ref}} = -100$ ps) for benzaldehyde. The time-resolved ratio patterns are those taken at $t =$ (a) -5 ps, (b) 0 ps, (c) $+5$ ps, (d) $+10$ ps, (e) $+20$ ps, (f) $+30$ ps, (g) $+40$ ps, (h) $+50$ ps, (i) $+100$ ps, (j) $+1000$ ps.

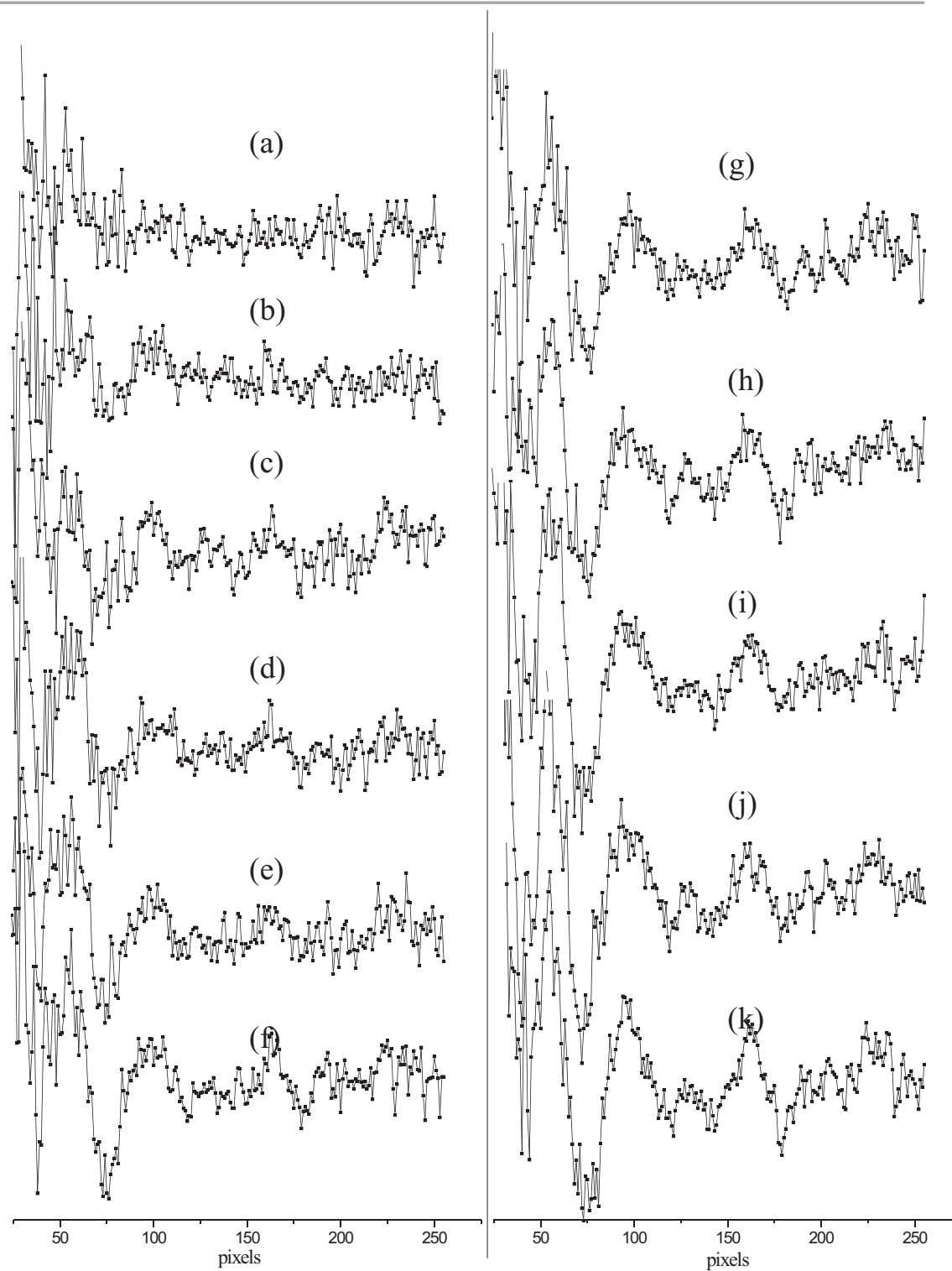


Fig. 7-3. The raw benzaldehyde difference data, $R^N(\text{pix})$, with $t_{\text{ref}} = -100$ ps. The time points are $t =$ (a) -5 ps, (b) 0 ps, (c) $+5$ ps, (d) $+10$ ps, (e) $+15$ ps, (f) $+20$ ps, (g) $+30$ ps, (h) $+40$ ps, (i) $+50$ ps, (j) $+100$ ps, (k) $+1000$ ps.

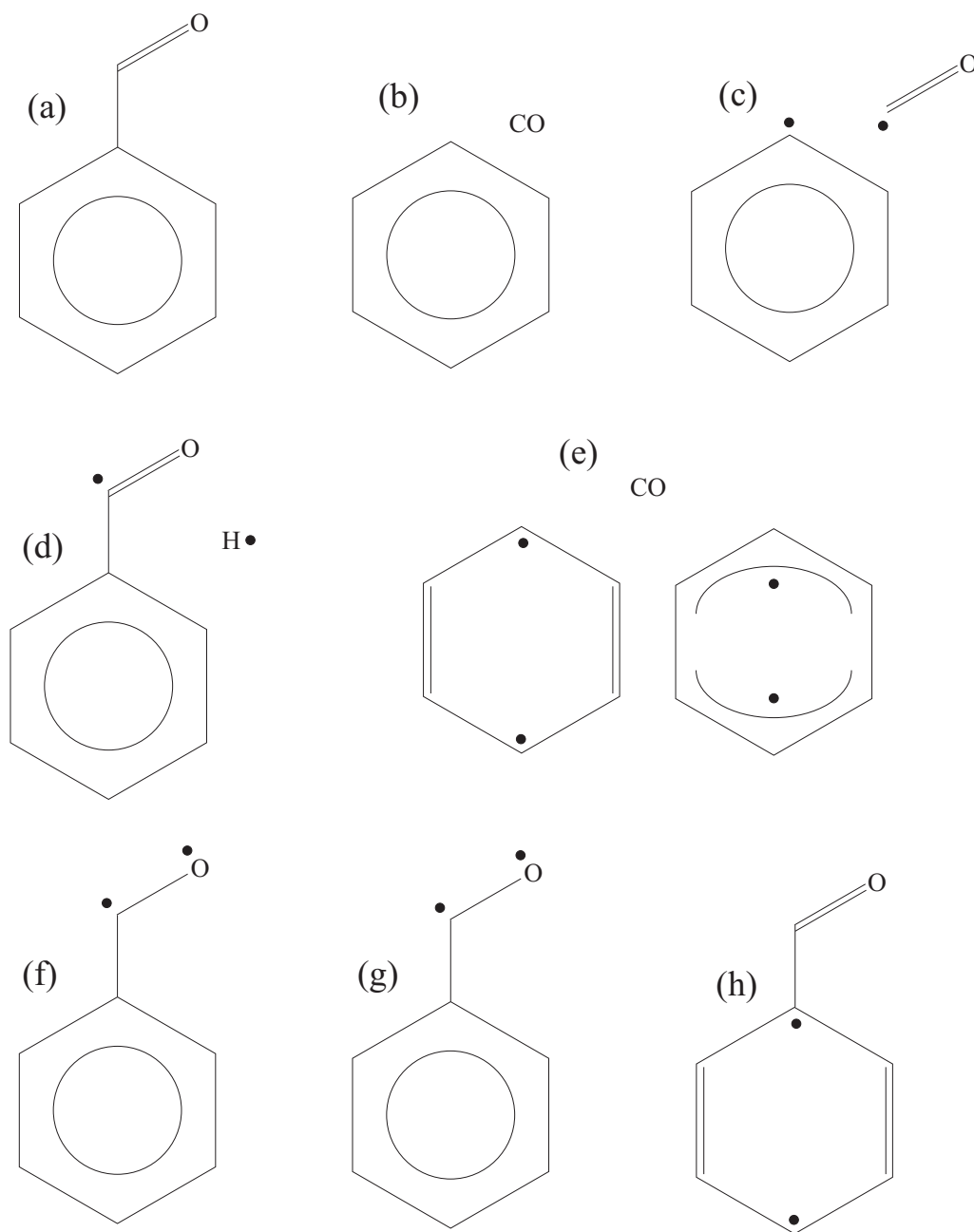


Fig. 7-4. Possible structures involved in the photolysis of benzaldehyde. (a) S_0 benzaldehyde, (b) benzene + CO, (c) phenyl + formyl radicals, (d) benzoyl radical + $H\bullet$, (e) T_1 * benzene (quinoid and anti-quinoid) + CO, (f) S_1 n * benzaldehyde, (g) T_1 n * benzaldehyde, (h) T_2 * benzaldehyde.

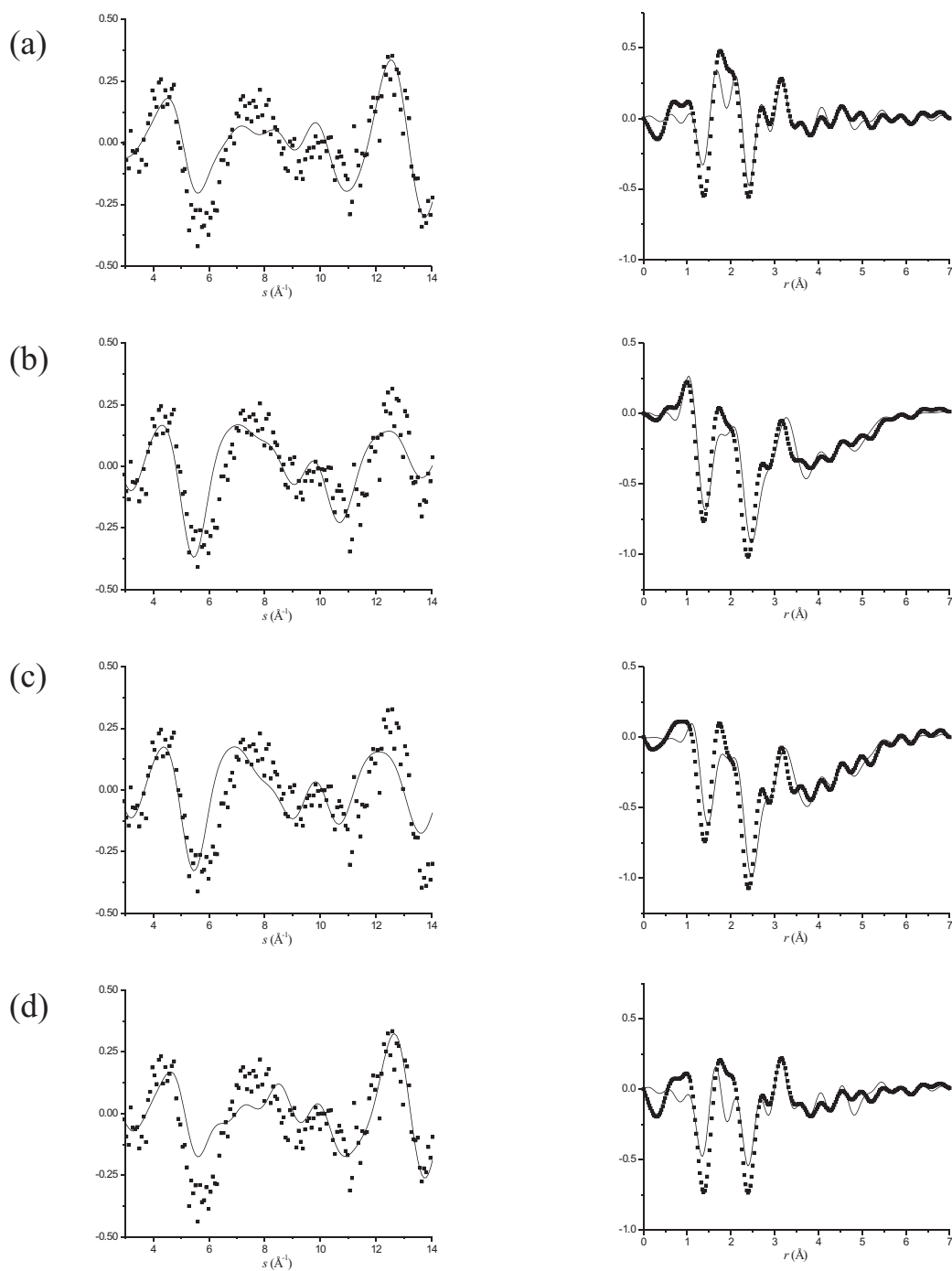


Fig. 7-5. Single-product channel comparisons between theory (solid line) and experimental (squares) $sM(s)$ (left column) and $f(r)$ (right column) curves ($t = +50$ ps; $t_{\text{ref}} = -100$ ps). Theory corresponds to the structures calculated for channels producing: (a) hot S_0 benzaldehyde, (b) benzene + CO, (c) phenyl + formyl radicals, (d) benzoyl radical + H. See text and Table 7-3 for details.

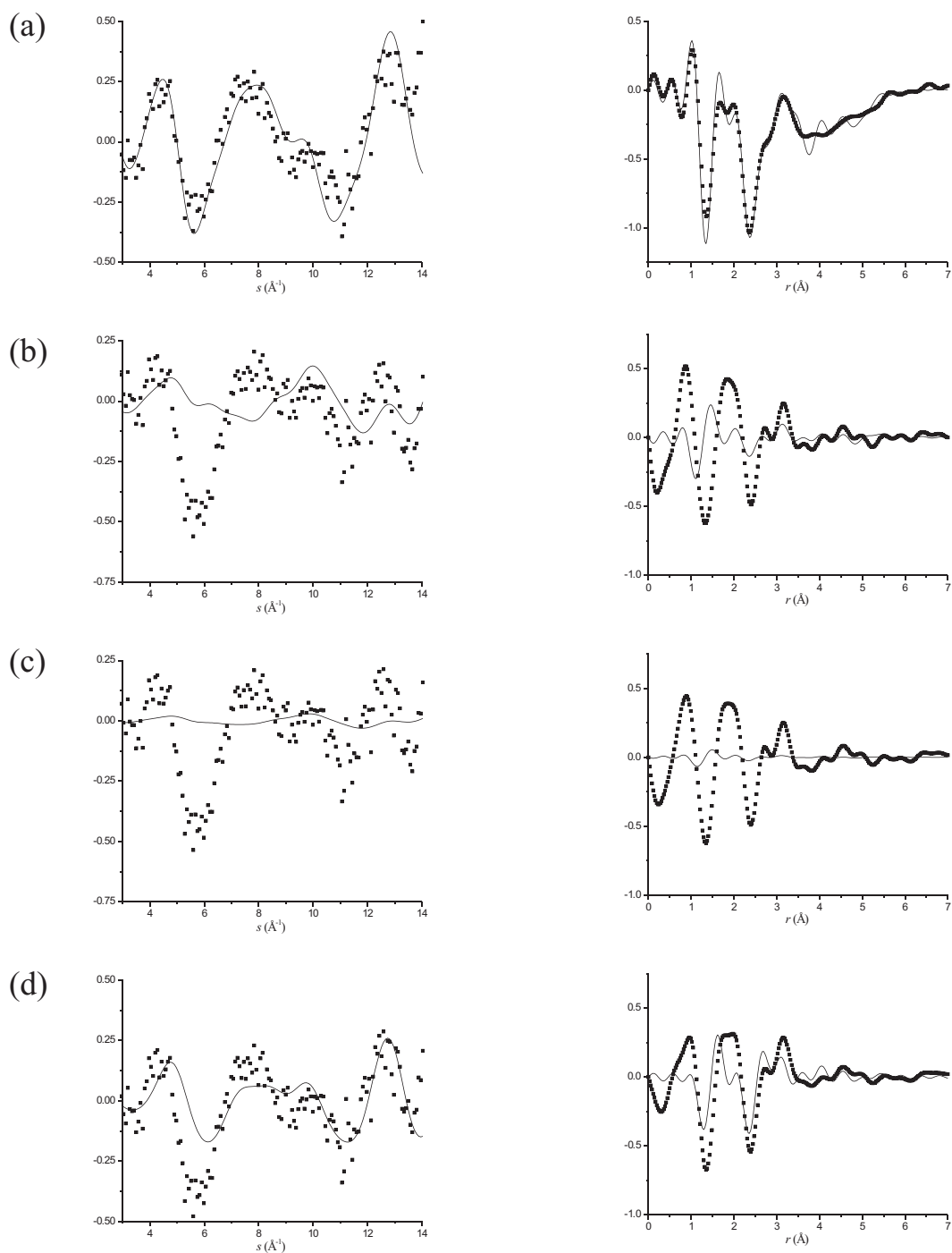


Fig. 7-6. Single-product channel comparisons between theory (solid line) and experimental (squares) $sM(s)$ (left column) and $f(r)$ (right column) curves ($t = +50$ ps; $t_{\text{ref}} = -100$ ps). Theory corresponds to the structures calculated for channels producing: (a) T_1 benzene (quinoid and anti-quinoid) + CO, (b) T_1 benzaldehyde, (c) S_1 benzaldehyde, (d) T_2 benzaldehyde. See text and Table 7-3 for details.

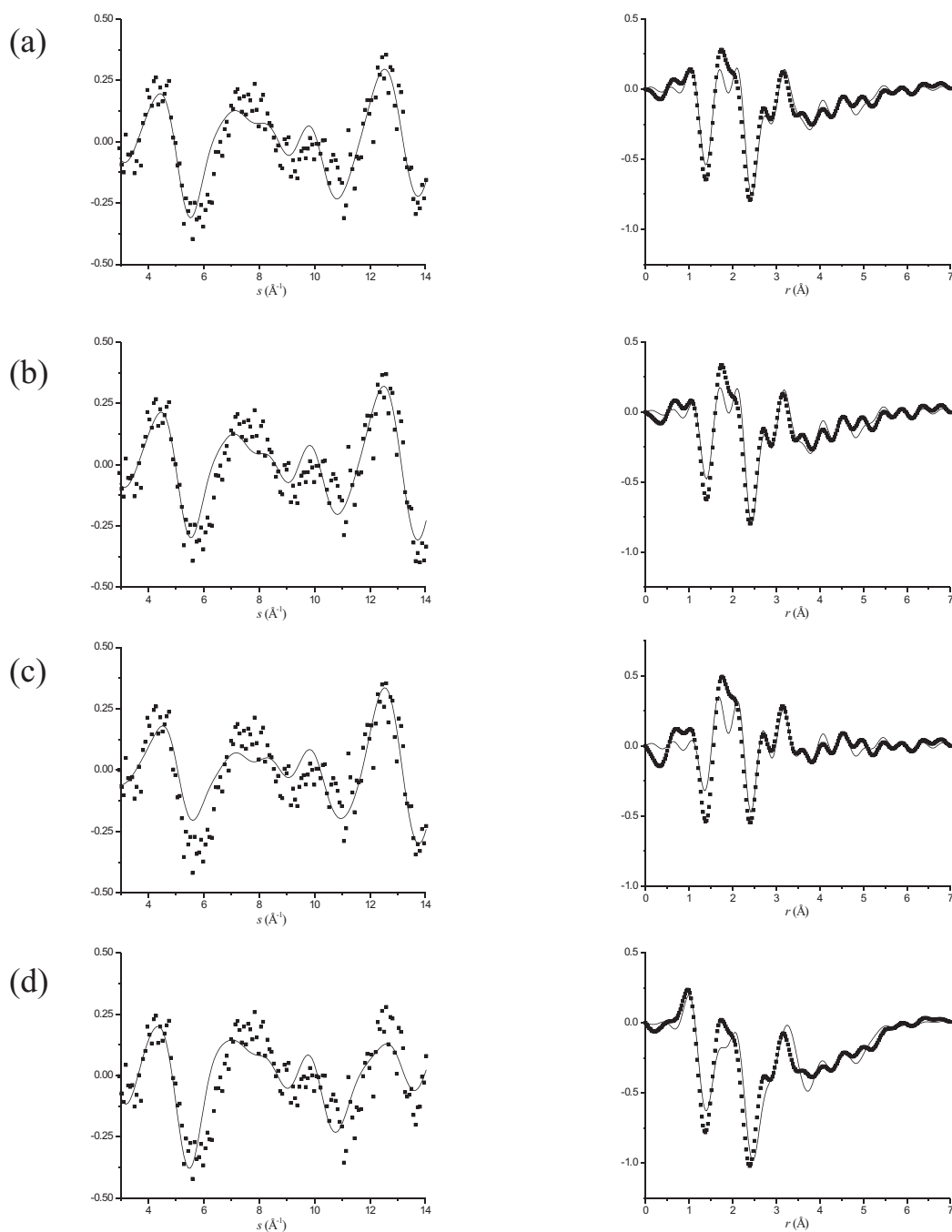


Fig. 7-7. Two-product channel comparisons between theory (solid line) and experimental (squares) $sM(s)$ (left column) and $f(r)$ (right column) curves ($t = +50$ ps; $t_{\text{ref}} = -100$ ps). Theory corresponds to the structures calculated for channels producing: (a) hot S_0 benzaldehyde + benzene + CO, (b) hot S_0 benzaldehyde + phenyl + formyl radicals, (c) hot S_0 benzaldehyde + benzoyl radical + H, (d) T_1 benzaldehyde + benzene + CO. See text and Table 7-4 for details.

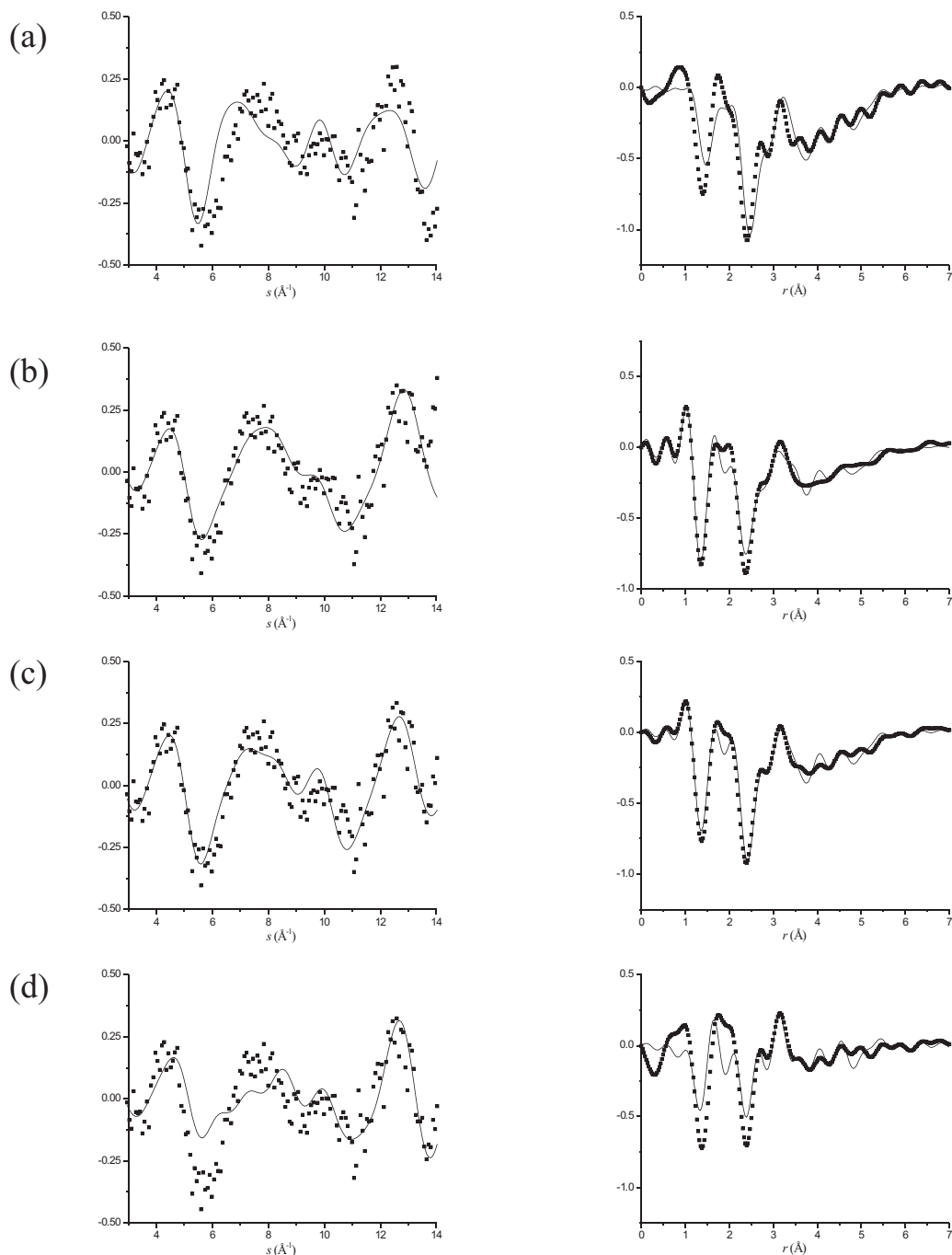


Fig. 7-8. Two-product channel comparisons between theory (solid line) and experimental (squares) $sM(s)$ (left column) and $f(r)$ (right column) curves ($t = +50$ ps; $t_{\text{ref}} = -100$ ps). Theory corresponds to the structures calculated for channels producing: (a) T_1 benzaldehyde + phenyl + formyl radicals, (b) T_1 benzaldehyde + T_1 benzene (quinoid + antiquinoid) + CO, (c) T_2 benzaldehyde + benzene + CO, (d) T_2 benzaldehyde + benzoyl radical + H. See text and Table 7-4 for details.

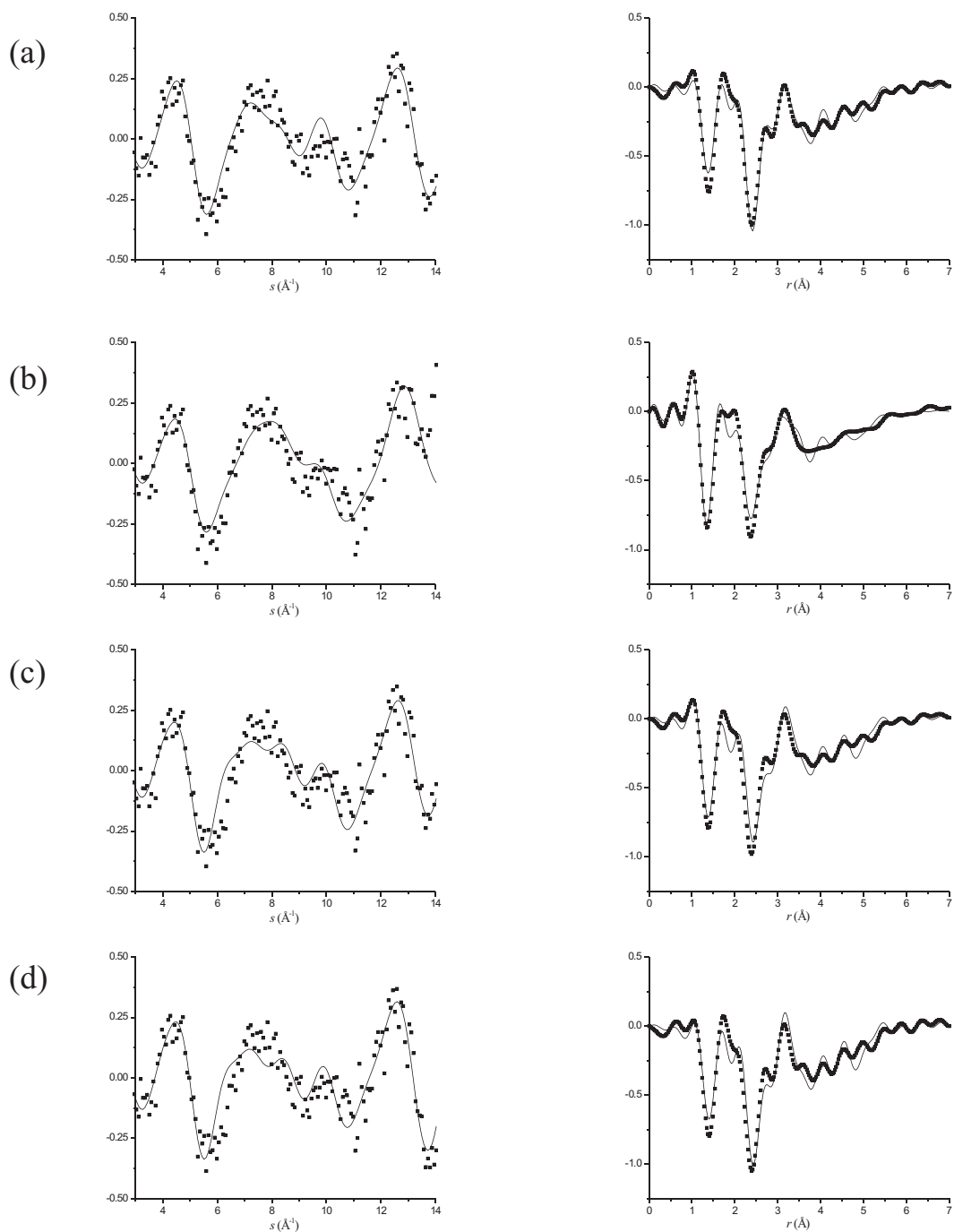


Fig. 7-9. Two-product channel comparisons between theory (solid line) and experimental (squares) $sM(s)$ (left column) and $f(r)$ (right column) curves ($t = +50$ ps; $t_{\text{ref}} = -100$ ps). Theory corresponds to the structures calculated for channels producing: (a) T_2 benzaldehyde + phenyl + formyl radicals, (b) T_2 benzaldehyde + T_1 benzene (quinoid + antiquinoid) + CO, (c) benzoyl radical + H + benzene + CO, (d) benzoyl radical + H + phenyl + formyl radicals. See text and Table 7-4 for details.

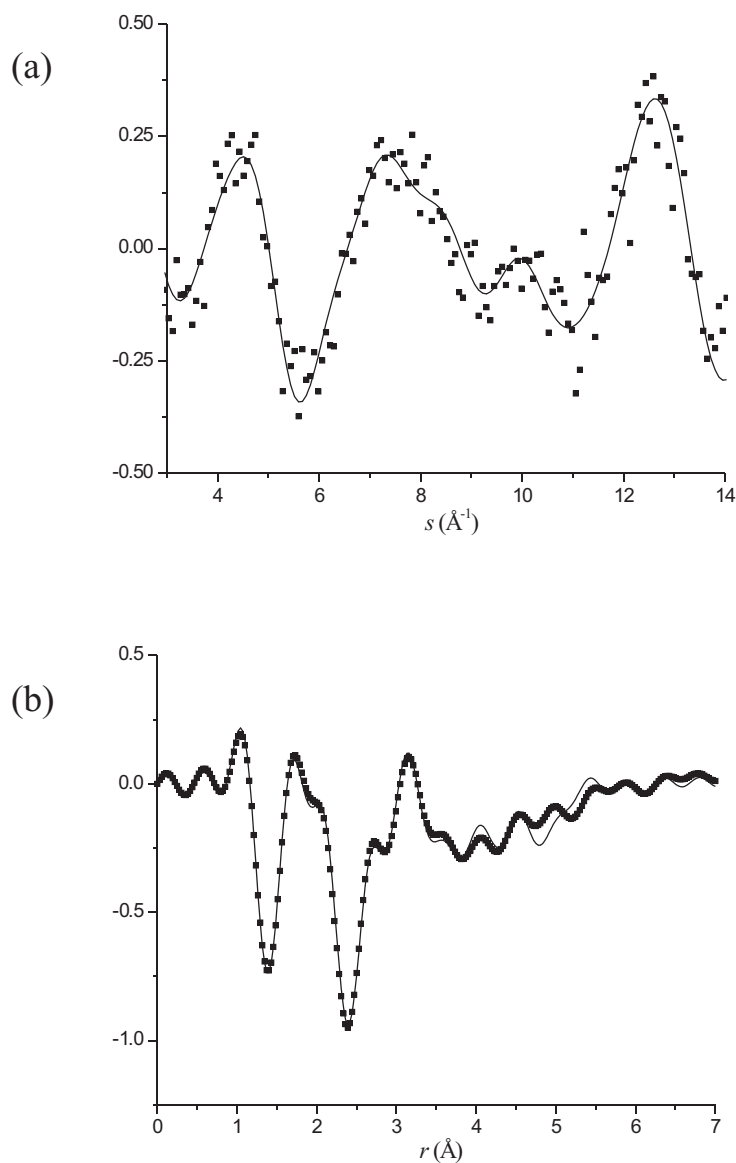


Fig. 7-10. The final refined theory (solid line) of the benzaldehyde decay channel producing T_2 benzaldehyde, benzene, and carbon monoxide with the experimental data (squares). (a) $sM(s)$ and (b) $f(r)$ curves correspond to $t = +50$ ps with $t_{\text{ref}} = -100$ ps. $\chi^2 = 2.101$; $R = 0.404$. See text for the structural model details and Table 7-5 for the refined structures.

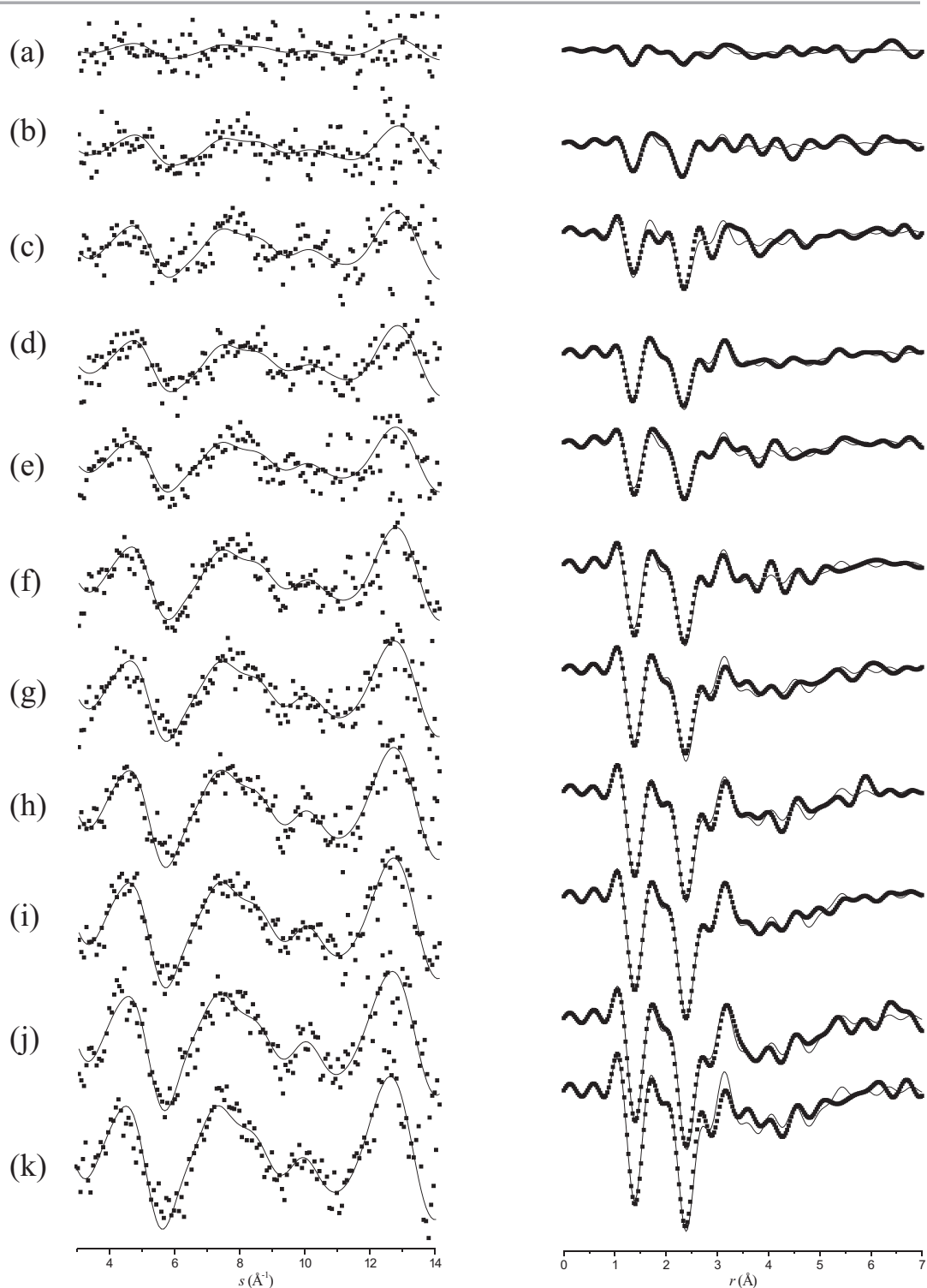


Fig. 7-11. The $sM(s)$ (left) column and $f(r)$ (right column) comparing the refined theory (solid) to the experimental data (squares) at time points $t =$ (a) -5 ps, (b) 0 ps, (c) $+5$ ps, (d) $+10$ ps, (e) $+15$ ps, (f) $+20$ ps, (g) $+30$ ps, (h) $+40$ ps, (i) $+50$ ps, (j) $+100$ ps, (k) $+1000$ ps. See Table 7-6 for details.

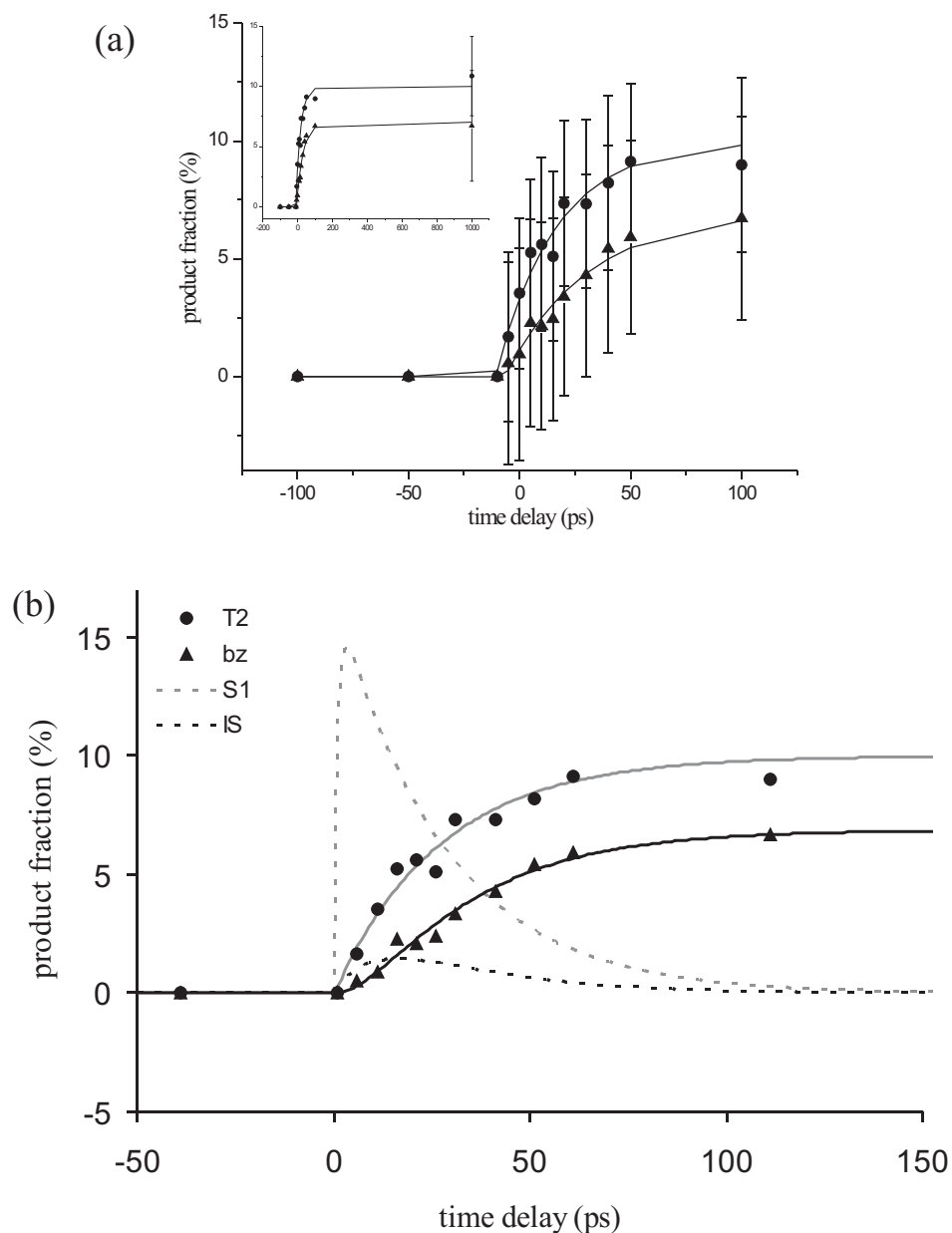


Fig. 7-12. The kinetics of the photophysical and photochemical channels of excited benzaldehyde. (a) The optimized fractional contributions of the product channels at each time point. A single-step reaction fit to each channel (solid line) gives apparent rise-time constants of 25 ps and 38 ps for the photophysical and photochemical products, respectively. (b) The kinetic model showing the rise of each product structure in the context of the other involved states in the bifurcation process. See text for details.

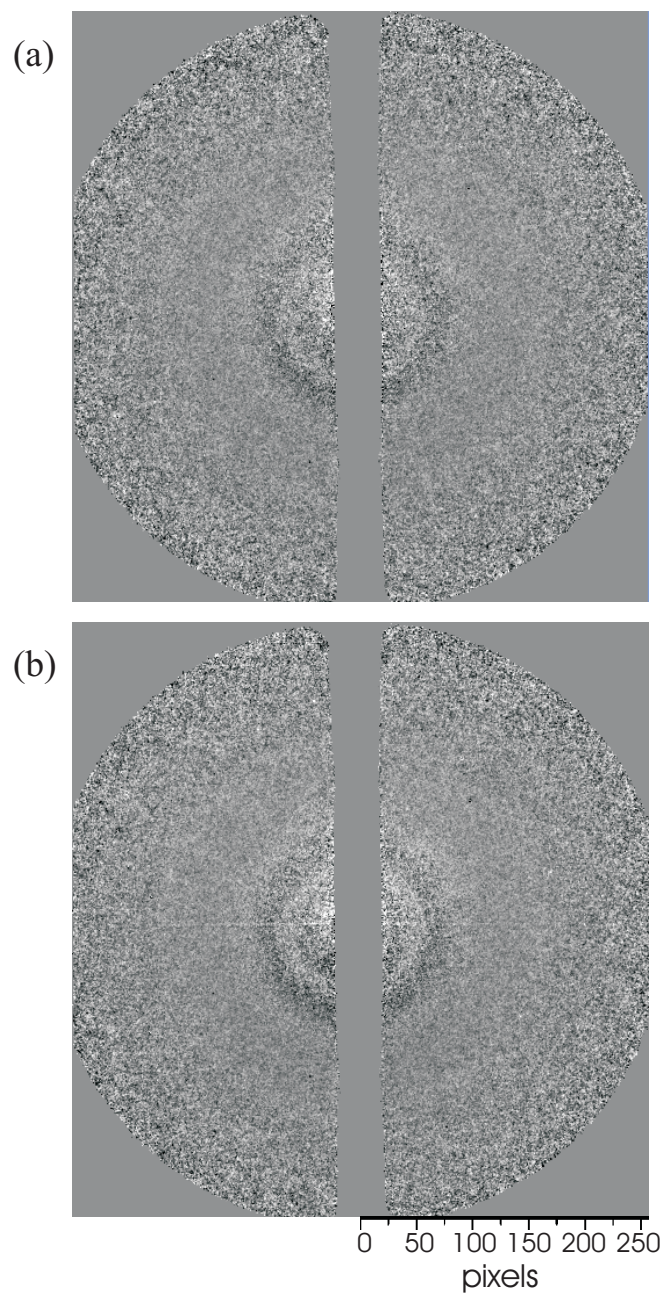


Fig. 7-13. The frame-referenced difference patterns ($t_{\text{ref}} = -100$ ps) for acetophenone. The time-resolved ratio patterns are those taken at $t =$ (a) +50 ps and (b) +100 ps from which the reference pattern is subtracted.

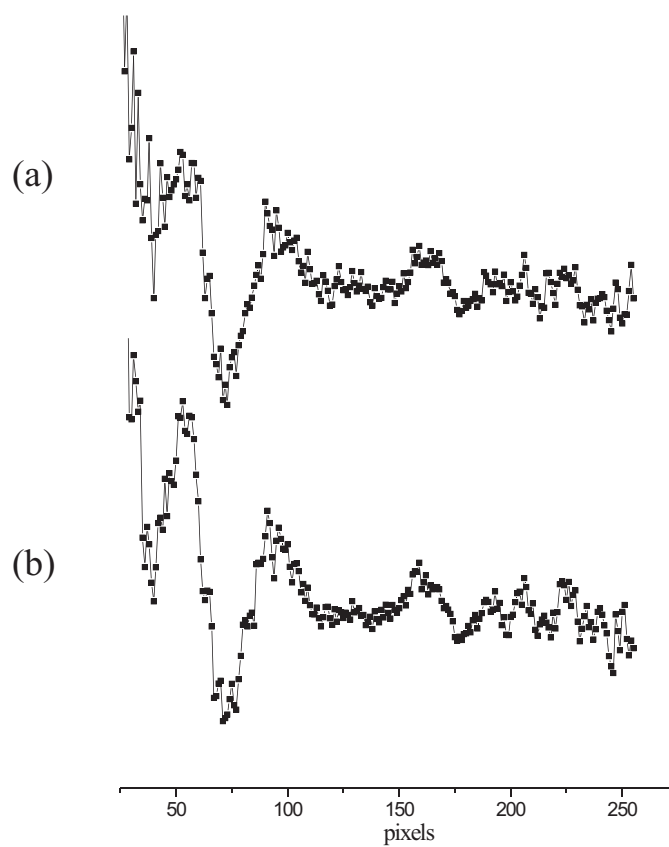


Fig. 7-14. The raw acetophenone difference data, $R^N(\text{pix})$, with $t_{\text{ref}} = -100$ ps. The time points are $t =$ (a) +50 ps and (b) +100 ps.

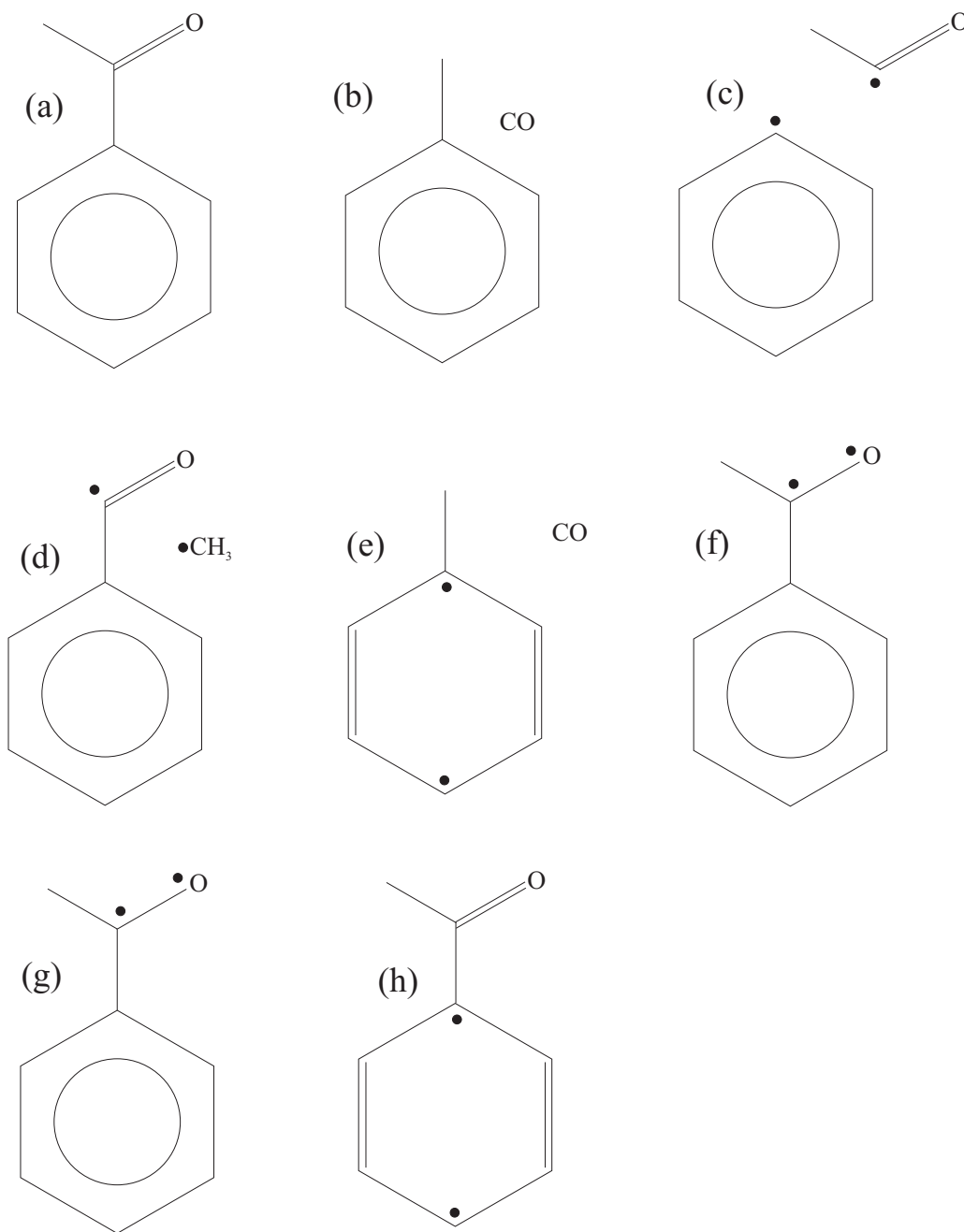


Fig. 7-15. Possible structures involved in the photolysis of acetophenone (a) S_0 acetophenone (b) toluene + CO, (c) phenyl + acetyl radicals, (d) benzoyl + methyl radicals, (e) T_1^* toluene + CO, (f) $S_1 n^*$ acetophenone (g) $T_1 n^*$ acetophenone, (h) T_2^* acetophenone.

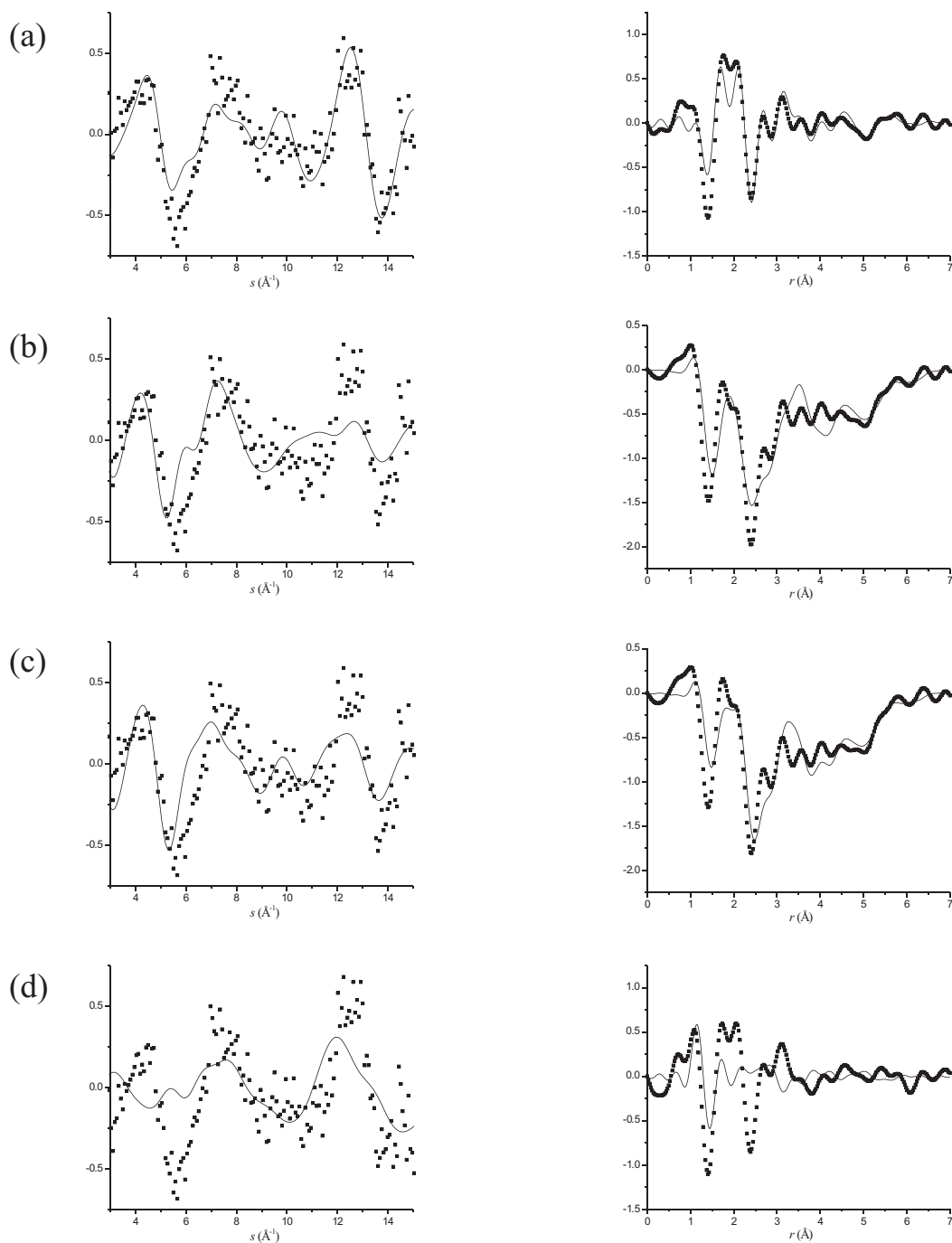


Fig. 7-16. Single-product channel comparisons between theory (solid line) and experimental (squares) $sM(s)$ (left column) and $f(r)$ (right column) curves for acetophenone ($t = +50$ ps; $t_{\text{ref}} = -100$ ps). Theory corresponds to the structures calculated for channels producing: (a) hot S_0 acetophenone, (b) benzoyl + methyl radicals, (c) phenyl + acetyl radicals, (d) S_1 acetophenone. See text and Table 7-7 for details.

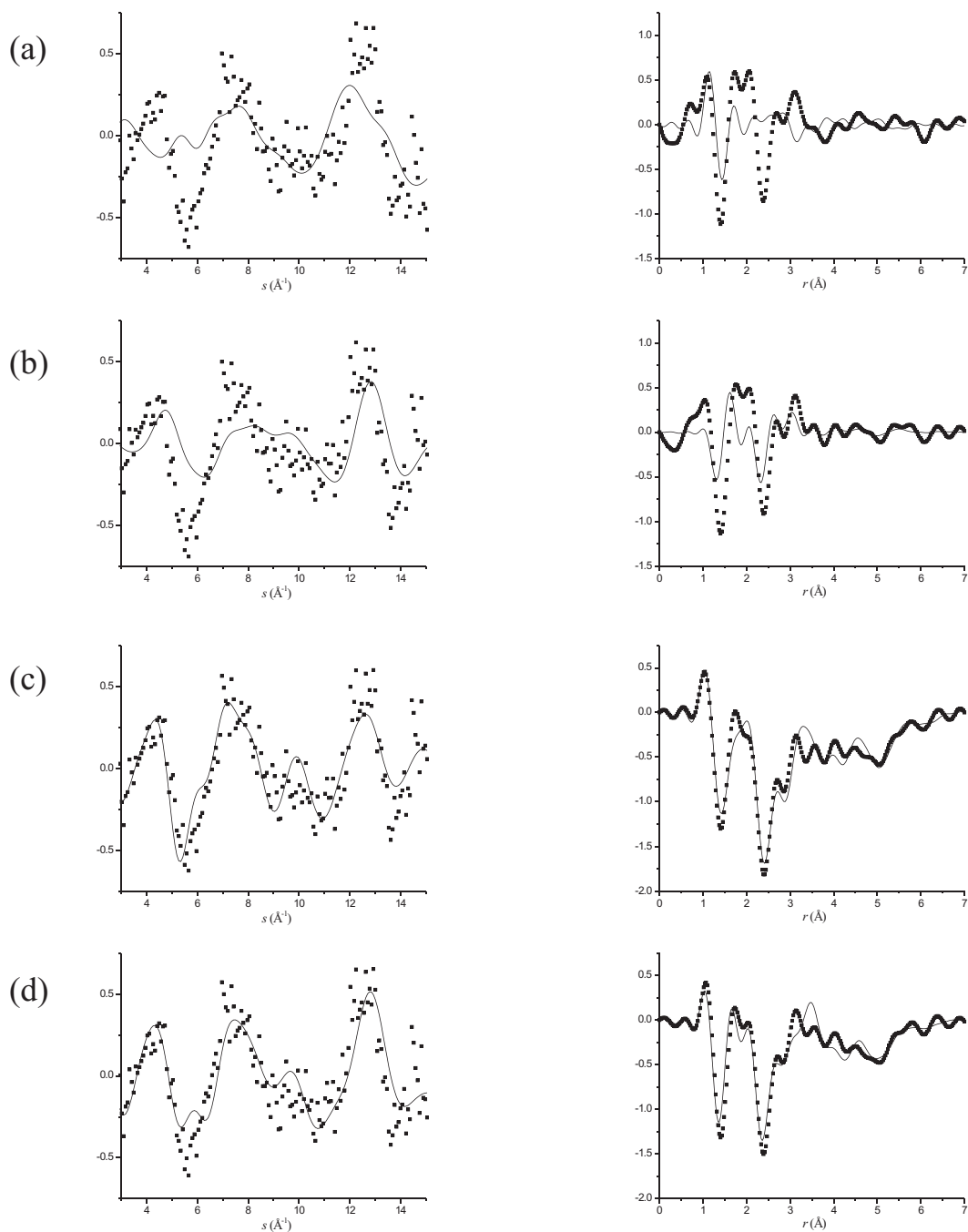


Fig. 7-17. Single-product channel comparisons between theory (solid line) and experimental (squares) $sM(s)$ (left column) and $f(r)$ (right column) curves for acetophenone ($t = +50$ ps; $t_{\text{ref}} = -100$ ps). Theory corresponds to the structures calculated for channels producing: (a) T_1 acetophenone, (b) T_2 acetophenone, (c) toluene + CO, (d) T_1 toluene + CO. See text and Table 7-7 for details.

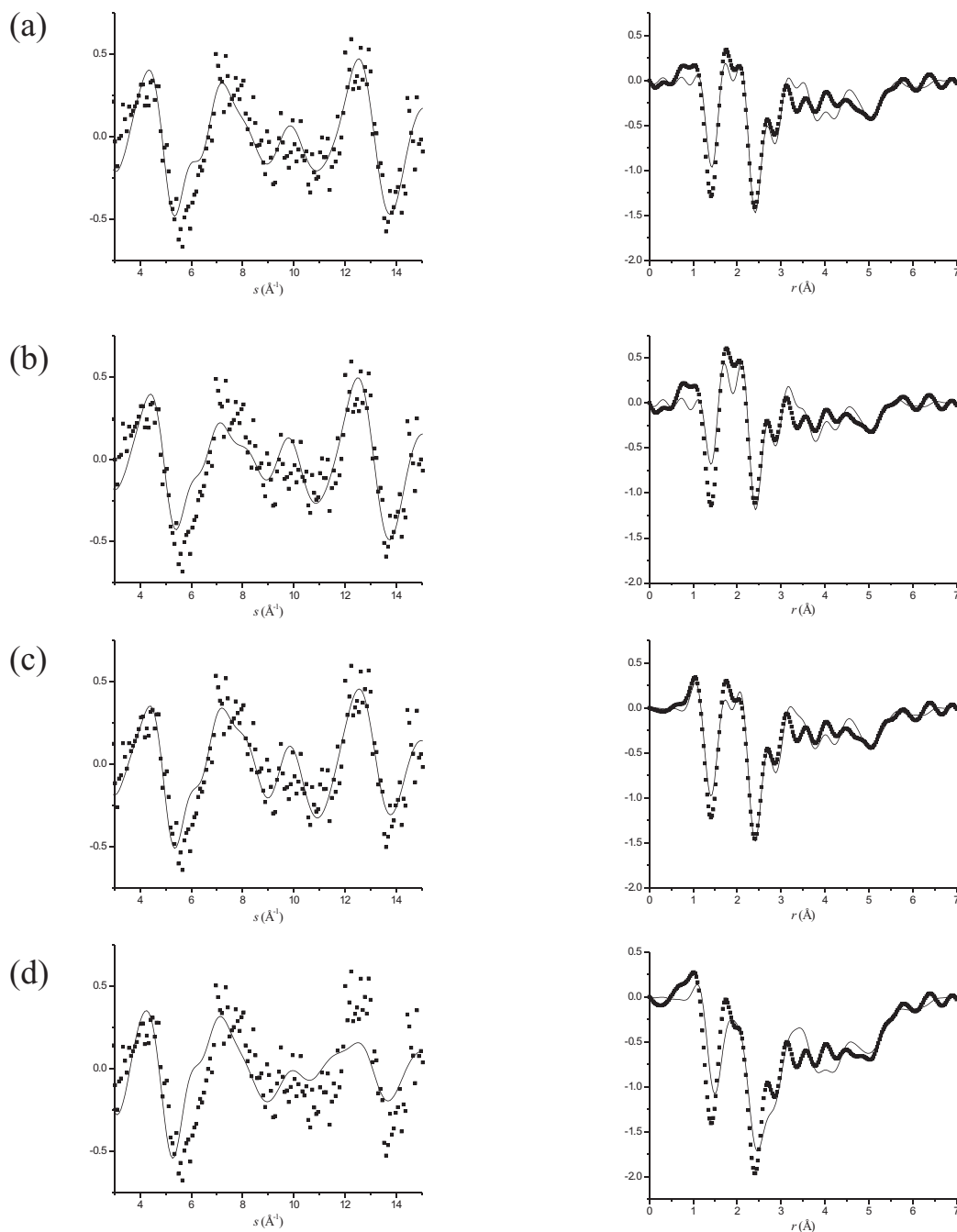


Fig. 7-18. Two-product channel comparisons between theory (solid line) and experimental (squares) $sM(s)$ (left column) and $f(r)$ (right column) curves for acetophenone ($t = +50$ ps; $t_{\text{ref}} = -100$ ps). Theory corresponds to the structures calculated for channels producing: (a) hot S_0 acetophenone and benzoyl + methyl radicals, (b) hot S_0 acetophenone and phenyl + acetyl radicals, (c) hot S_0 acetophenone and toluene + CO, (d) benzoyl + methyl + phenyl + acetyl radicals. See text and Table 7-8 for details.

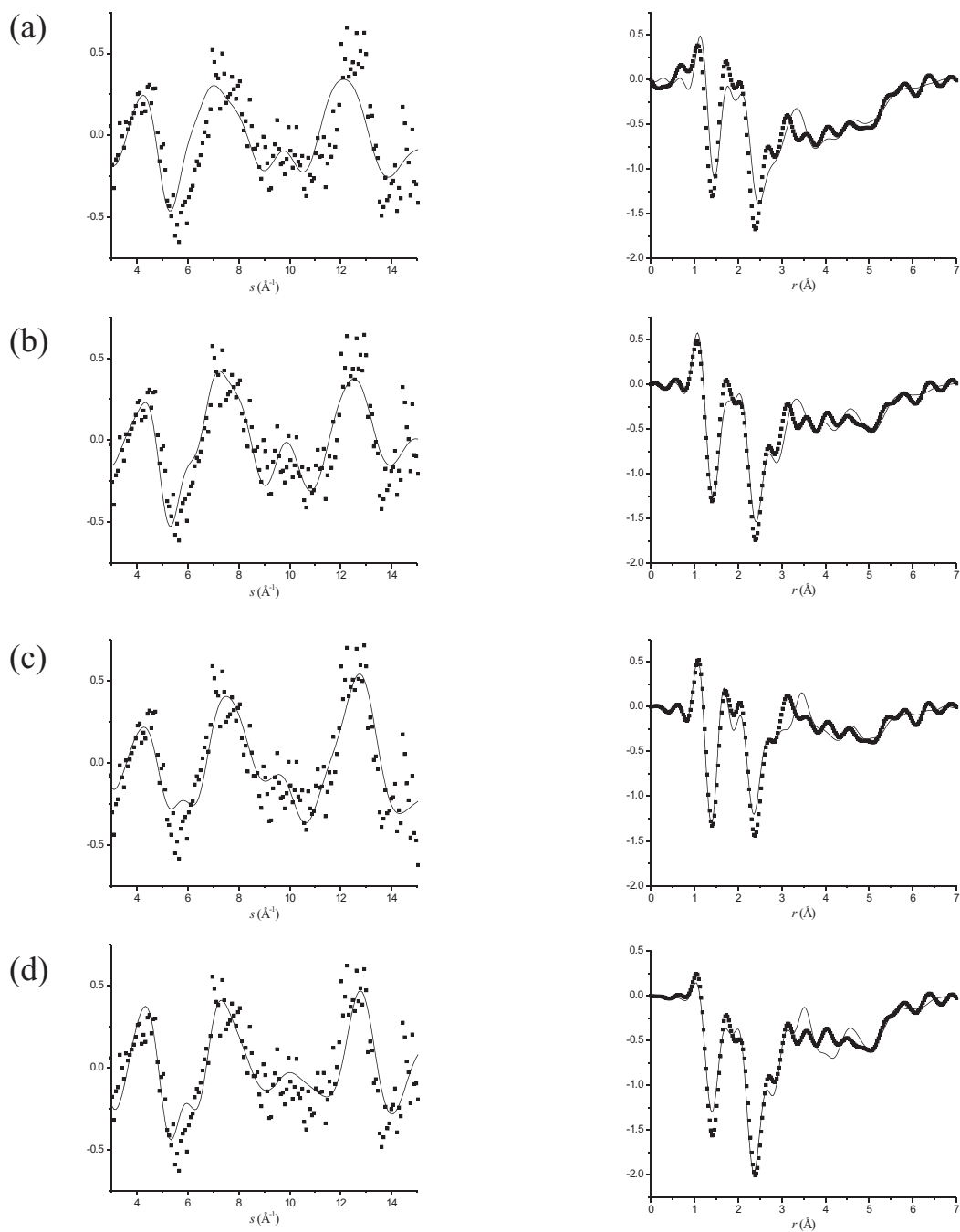


Fig. 7-19. Two-product channel comparisons between theory (solid line) and experimental (squares) $sM(s)$ (left column) and $f(r)$ (right column) curves for acetophenone ($t = +50$ ps; $t_{\text{ref}} = -100$ ps). Theory corresponds to the structures calculated for channels producing: (a) T_1 acetophenone and phenyl + acetyl radicals, (b) T_1 acetophenone and toluene + CO, (c) T_1 acetophenone and T_1 toluene + CO, (d) T_2 acetophenone + benzoyl + methyl radicals. See text and Table 7-8 for details.

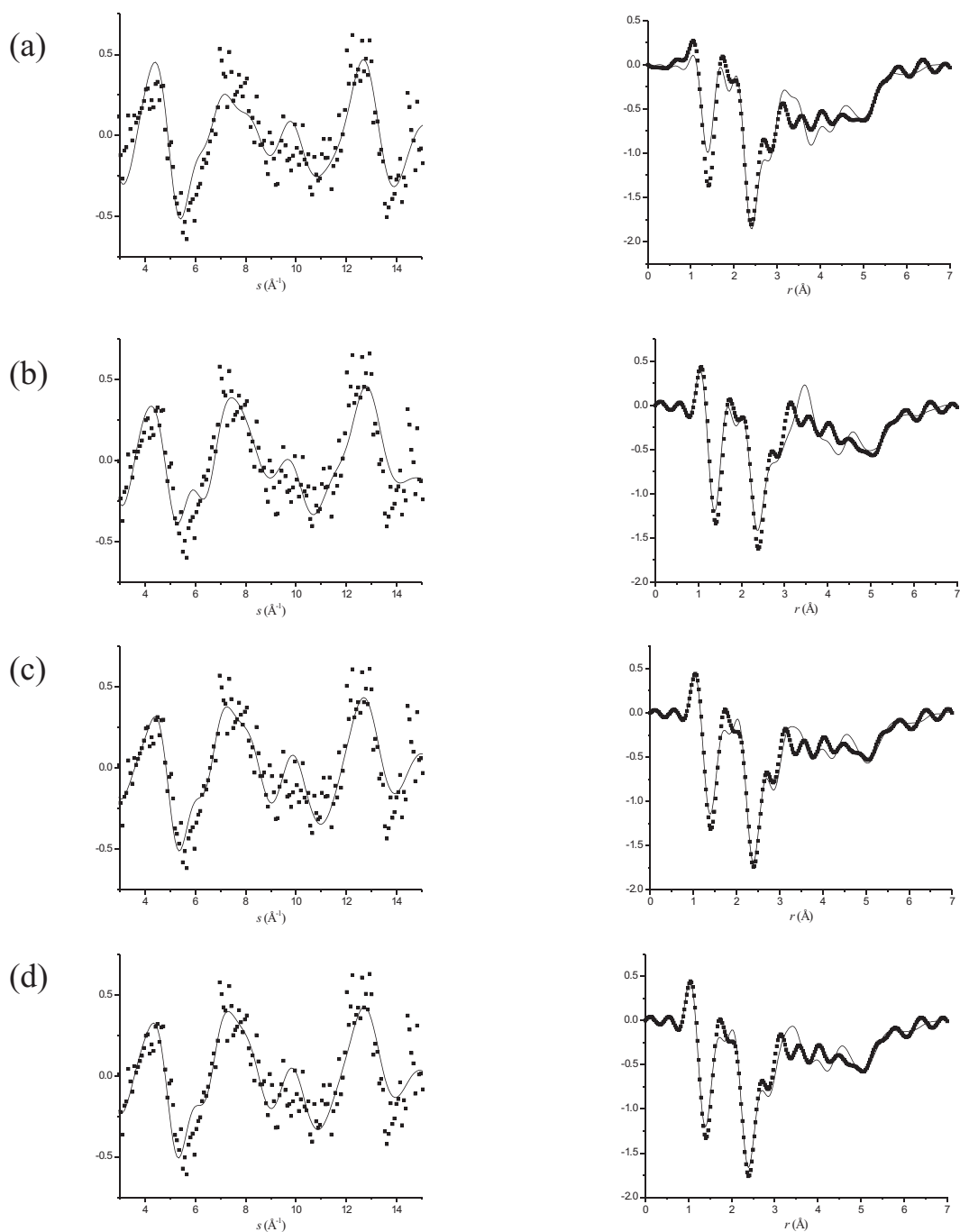


Fig. 7-20. Two-product channel comparisons between theory (solid line) and experimental (squares) $sM(s)$ (left column) and $f(r)$ (right column) curves for acetophenone ($t = +50$ ps; $t_{\text{ref}} = -100$ ps). Theory corresponds to the structures calculated for channels producing: (a) T_2 acetophenone and phenyl + acetyl radicals, (b) T_2 acetophenone and T_1 toluene + CO, (c) T_2 acetophenone and toluene + CO, (d) T_1 toluene + CO and toluene + CO. See text and Table 7-8 for details.

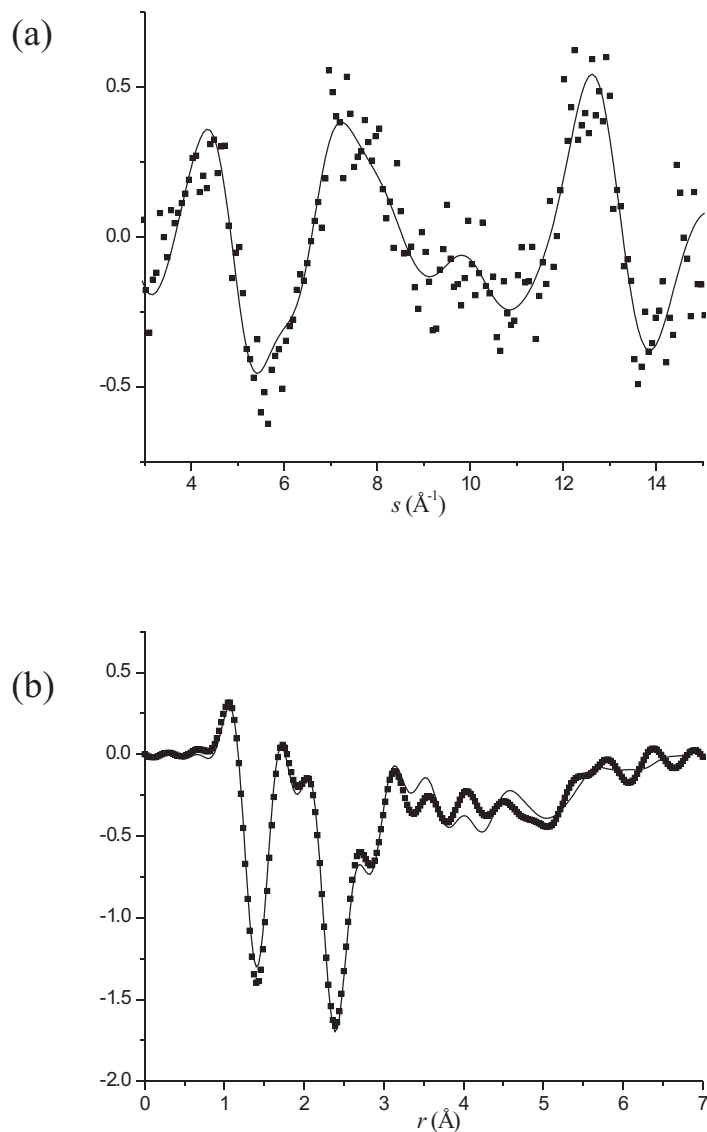


Fig. 7-21. The (a) $sM(s)$ and (b) $f(r)$ of the final refined theory (solid line) and the experimental data for the decay products of acetophenone at +50 ps ($t_{\text{ref}} = -100$ ps). The product structures correspond the photophysical and photochemical pathways producing T_2 acetophenone and benzoyl + methyl radicals, respectively. $\chi^2 = 4.841$; $R = 0.473$. See text for details and Table 7-9 for the refined geometries of the products.

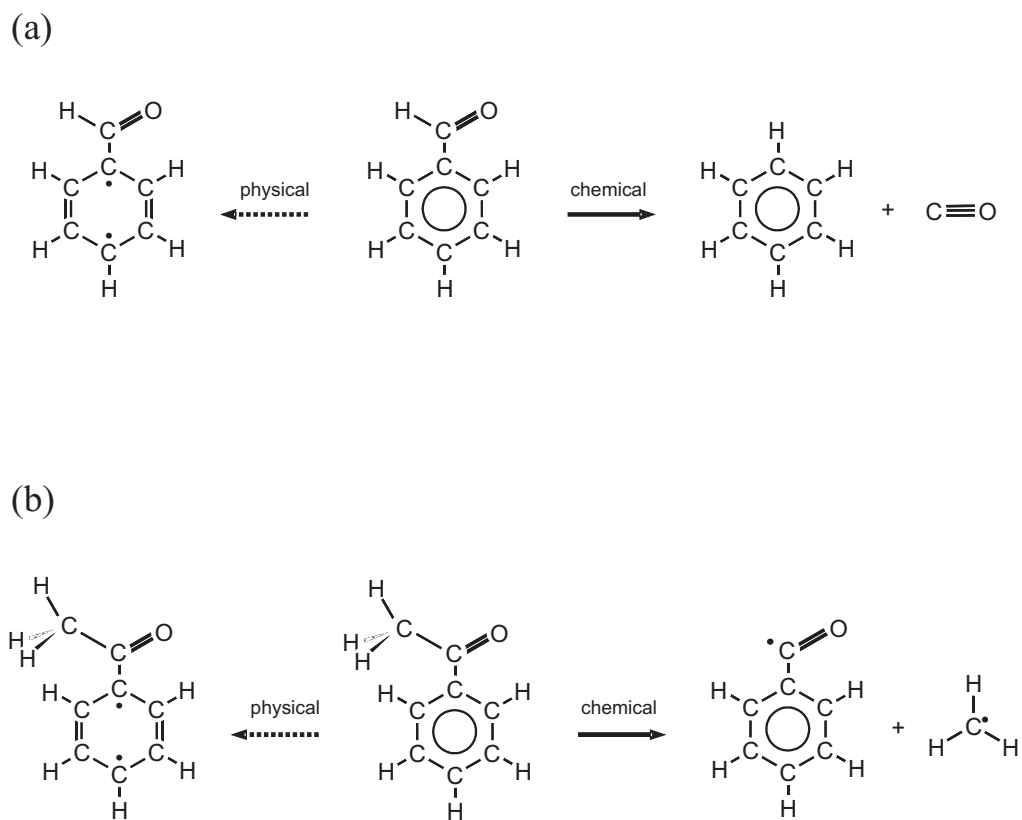


Fig. 7-22. The schematic structures of the photophysical and photochemical processes of (a) benzaldehyde and (b) acetophenone as resolved by UED.

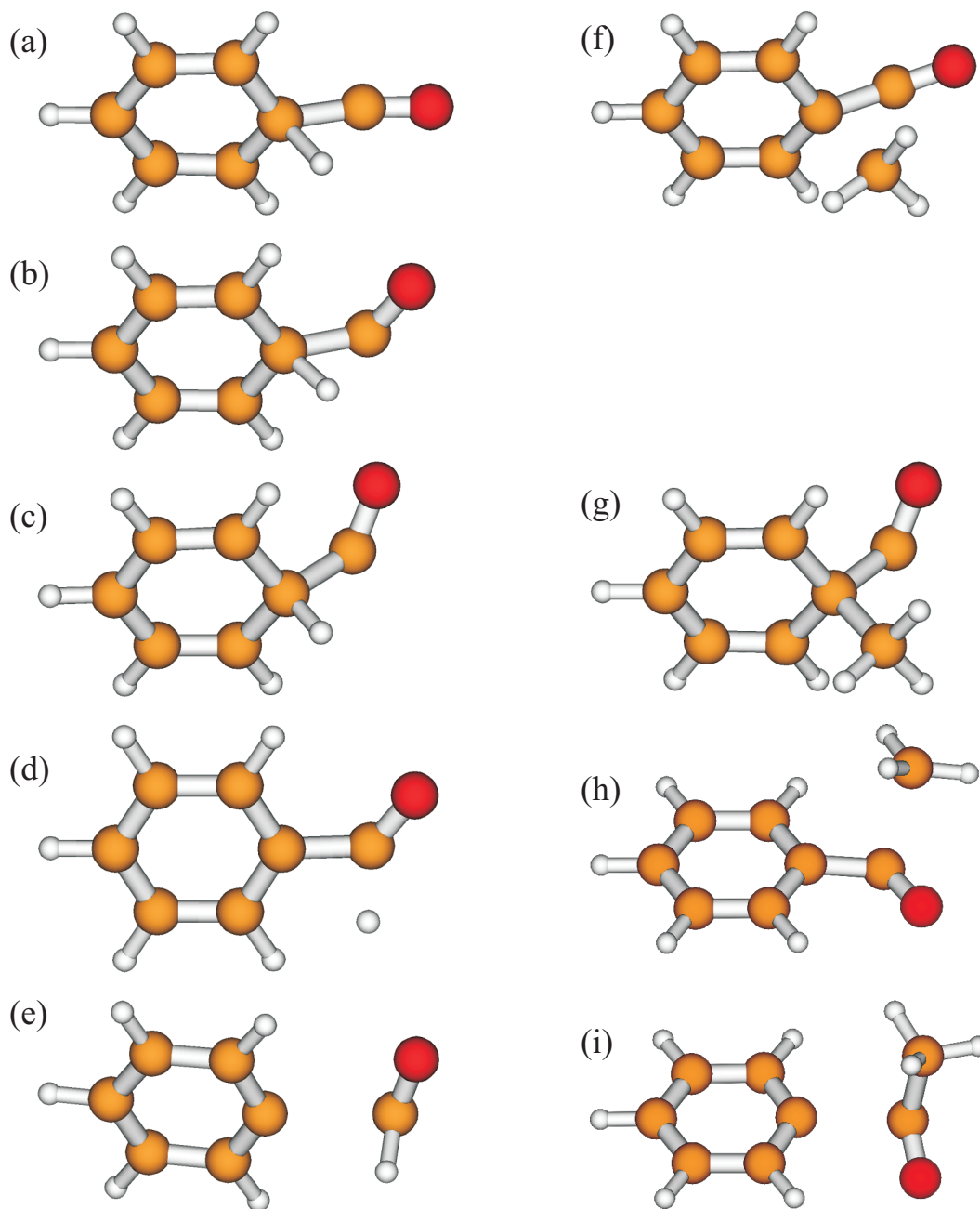


Fig. 7-23. The structures of some transition states (TS) and intermediates (IS) in various theoretical reaction schemes of benzaldehyde (left column) and acetophenone (right column). (a) the TS for the loss of CO from S_0 , (b) the TS for the loss of CO from n^* , (c) the IS for the loss of CO from n^* , (d) the TS for the loss of H from n^* , (e) the TS for the loss of acetyl from n^* , (f) the TS for the loss of CO from S_0 , (g) the IS for the loss of CO from n^* , (h) the TS for the loss of methyl from n^* , and (i) the TS for the loss of acetyl from n^* . Note that there is no TS for the loss of CO from n^* acetophenone.

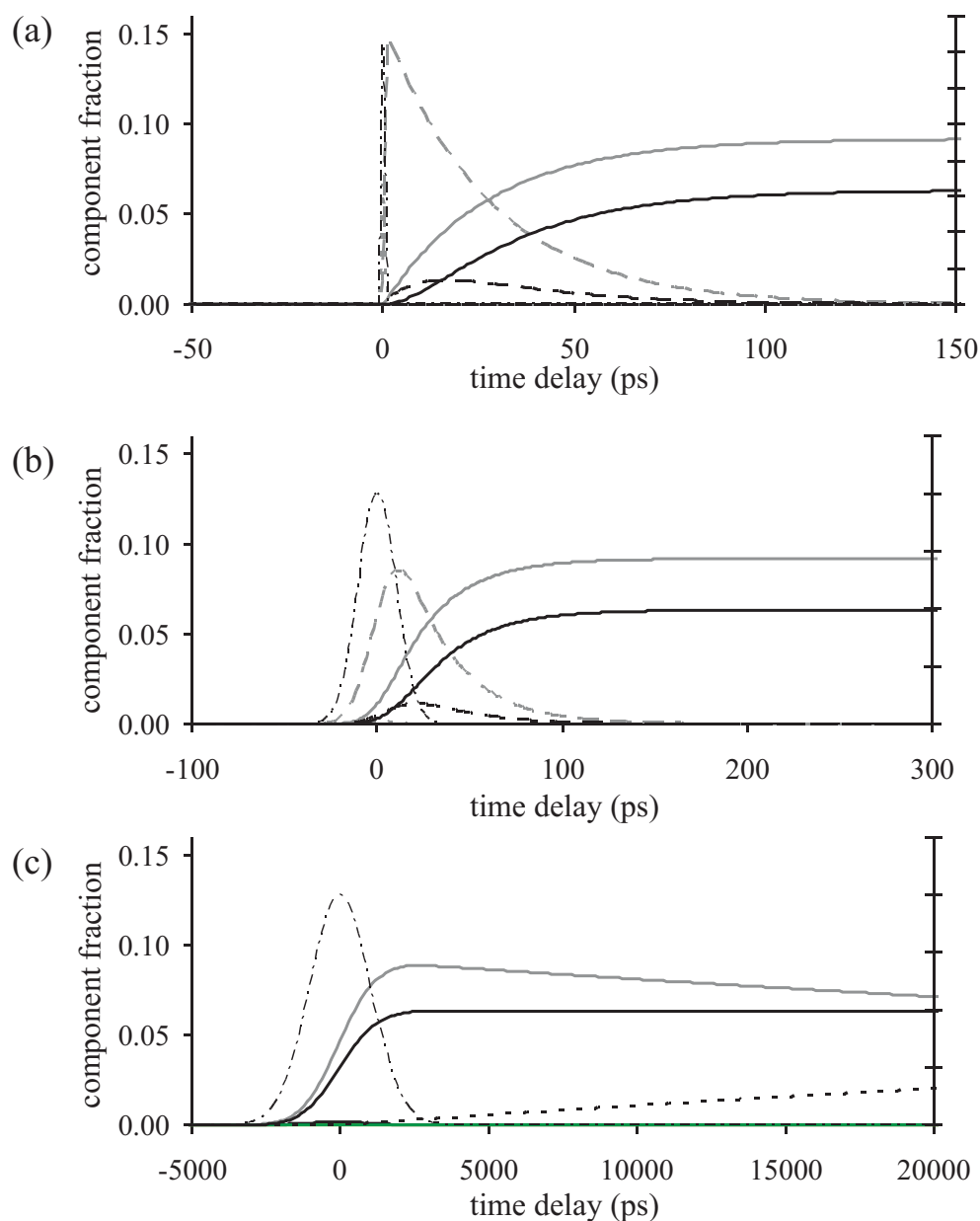


Fig. 7-24. The models of population flow upon 266.7 nm excitation of benzaldehyde. The lines denote difference states involved in the decay channels: (gray short dashed) S_2 , (gray long dashed) S_1 , (gray solid) T_2 , (black long dash) the intermediate state, (black solid) benzene + CO, (black short dash) T_1 benzene + CO, and (black dash dot) the excitation laser pulse. Each panel depicts the dynamics depending on the excitation laser pulse width, τ_1 . (a) $\tau_1 = 110$ fs, like UED, (b) $\tau_1 = 20$ ps, and (c) $\tau_1 = 2$ ns. The simulations show how different species are detectable depending on the time scale of the experiment.

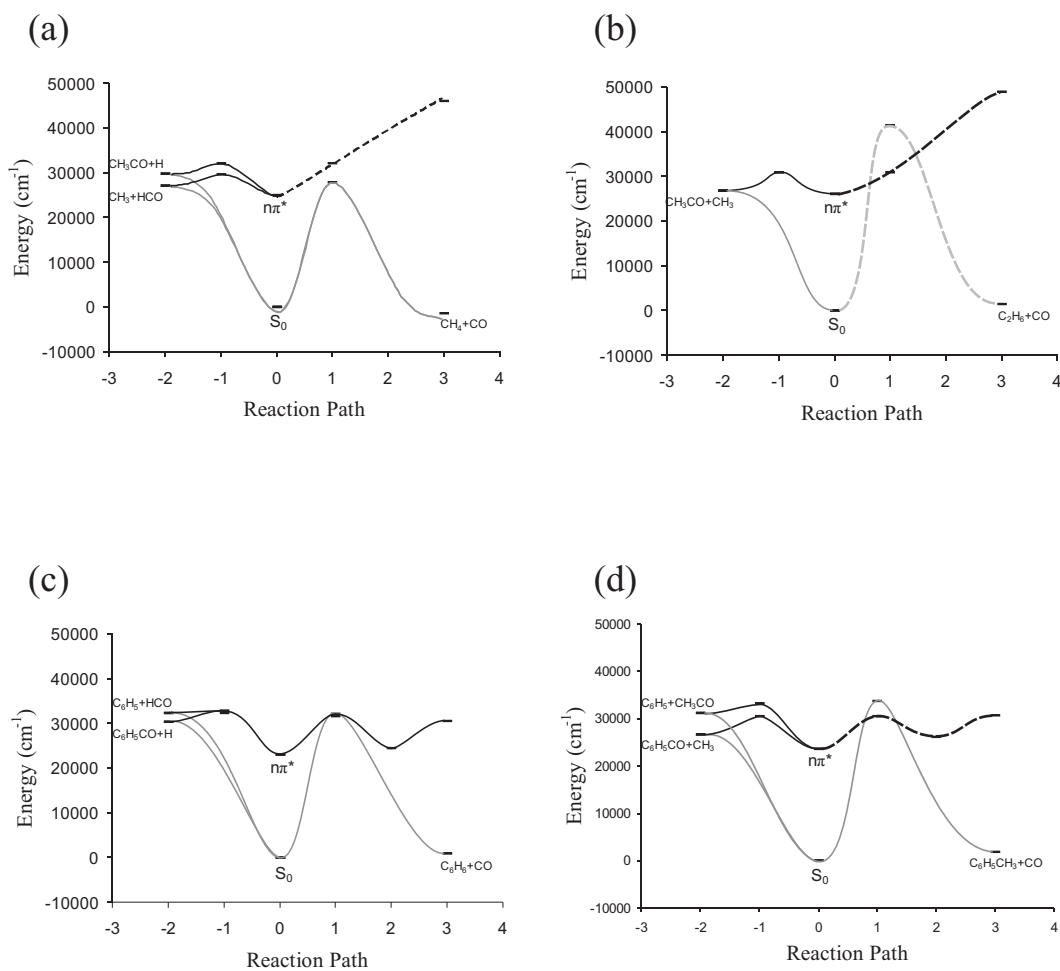


Fig. 7-25. Calculated reaction coordinates for radical cleavage and molecular dissociation reactions on the ground and $n\pi^*$ excited surfaces of (a) acetaldehyde, (b) acetone, (c) benzaldehyde, and (d) acetophenone. Dashed lines trace hypothetical reactions.

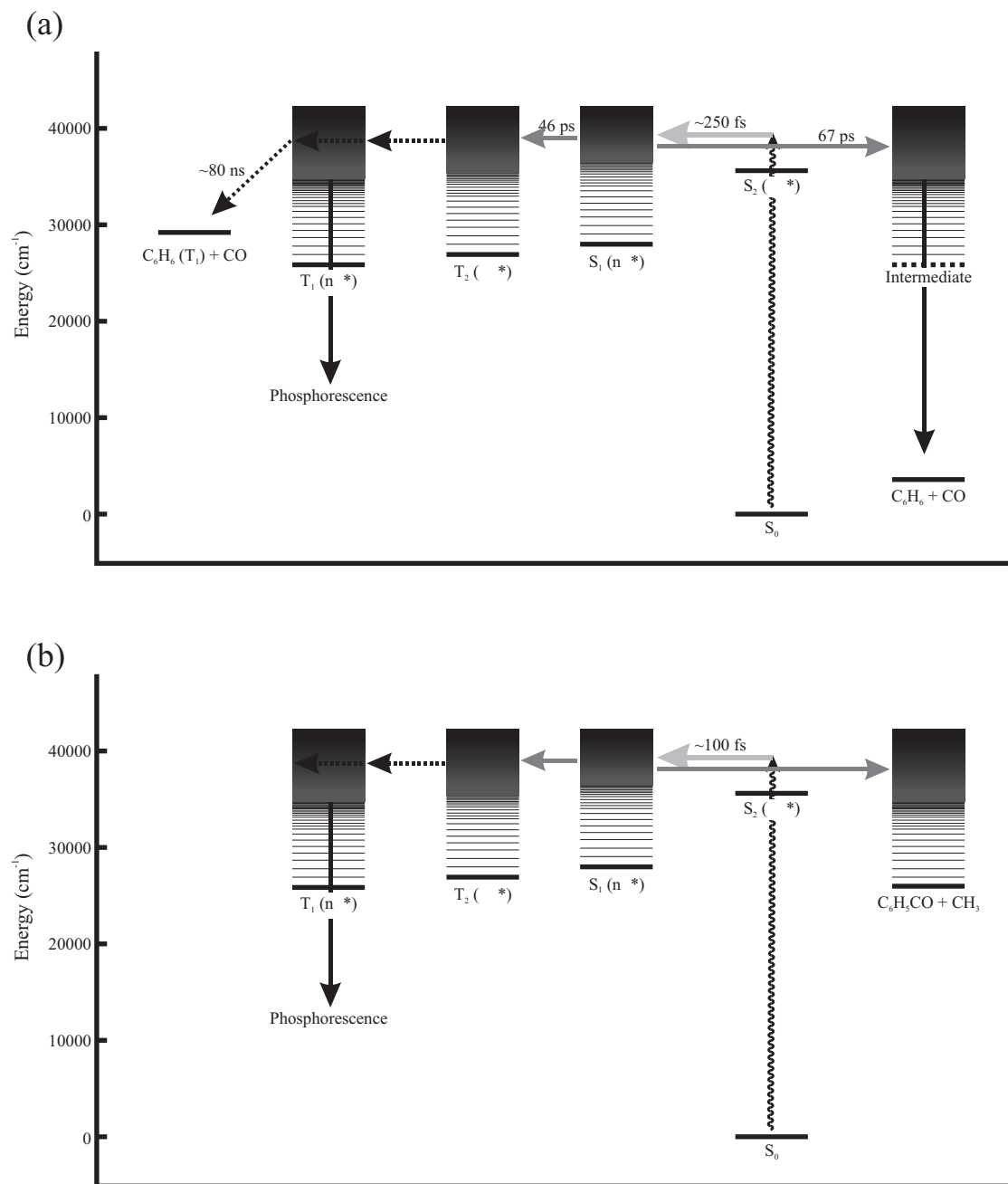


Fig. 7-26. Schematic illustration of the bifurcation into photophysical and photochemical pathways upon excitation of (a) benzaldehyde and (b) acetophenone.